

A Proposal for a Parameterized Circulating Vector Field Guidance for Fixed Wing
Unmanned Aerial Vehicles

A thesis presented to
the faculty of
the Russ College of Engineering and Technology of Ohio University

In partial fulfillment
of the requirements for the degree
Master of Science

Garrett S. Clem
December 2017
© 2017 Garrett S. Clem. All Rights Reserved.

This thesis titled

A Proposal for a Parameterized Circulating Vector Field Guidance for Fixed Wing
Unmanned Aerial Vehicles

by

GARRETT S. CLEM

has been approved for

the Department of Mechanical Engineering

and the Russ College of Engineering and Technology by

Jay P. Wilhelm

Assistant Professor of Mechanical Engineering

Dennis Irwin

Dean, Russ College of Engineering and Technology

ABSTRACT

CLEM, GARRETT S., M.S., December 2017, Mechanical Engineering

A Proposal for a Parameterized Circulating Vector Field Guidance for Fixed Wing

Unmanned Aerial Vehicles (34 pp.)

Director of Thesis: Jay P. Wilhelm

ABSTRACT

DED

ACKNOWLEDGMENTS

ACK

TABLE OF CONTENTS

	Page
Abstract	3
Dedication	4
Acknowledgments	5
List of Tables	7
List of Figures	8
List of Symbols	9
List of Acronyms	10
1 Introduction	11
1.1 Motivation and Problem Statement	11
1.2 Methods Overview	12
1.3 Phase I	12
1.4 Phase II	12
1.5 Phase III	12
1.6 Summary of Phases	13
2 Literature Review	14
2.1 Introduction to Literature Review	14
2.2 Unmanned Aerial Vehicle	14
2.3 Vector Field Guidance	16
2.3.1 Introduction to Vector Field Guidance	16
2.3.2 Potential Field	16
2.3.3 Lyapunov Vector Fields	20
2.3.4 Non-Lyapunov Vector Fields	24
2.3.5 Gradient Vector Field	26
2.4 Unmanned Aerial Vehicle Simulation	31
2.5 Literature Review Summary	32
References	33

LIST OF TABLES

Table	Page
-------	------

LIST OF FIGURES

Figure	Page
2.1 Unmanned Aerial System (UAS)	14
2.2 Autopilot's Navigation, Guidance, and Control Architecture	15
2.3 Single Obstacle Potential Field Gradient [5]	17
2.4 Virtual force field histogram acting on a mobile robot	18
2.5 Potential Field Local Minimum [5]	19
2.6 Potential Field Local Minimum [5]	19
2.7 Obstacle Clustering [5]	20
2.8 Lyapunov vector field for straight line and circular primitives	21
2.9	22
2.10 Lyapunov vector field approach curved path asymptotically	22
2.11 Elliptical VF produced by non-linear coordinate transformations a) [14] b) [15]	23
2.12 Tangent plus lyapunov vector fields for shortest path target tracking [17] . . .	24
2.13 RRT* path planner with a VF used as a task specification	25
2.14 Vector field within a set of constrained delaunay triangles [19]	25
2.15 Attractive vector field (a) and clockwise circulation field (b)	27
2.16 Repulsive vector field a) and counterclockwise circulation field b)	27
2.17 Place holder image of UAV following ground target	28
2.18	28
2.19	29
2.20 Dubins UAV actuator saturation	31
2.21 Differential drive mobile robot simulating fixed wing UAV Dubins constraints .	32

LIST OF SYMBOLS

a Previous or Initial Axial Induction Factor (-)

LIST OF ACRONYMS

AoA Angle of Attack

1 INTRODUCTION

1.1 Motivation and Problem Statement

Fixed wing Unmanned Aerial Vehicles (UAVs) are used for missions such as surveillance and reconnaissance that might put pilots in harms way [1]. Missions typically consist of sequential objectives represented as waypoints that the UAV follows. Waypoints may be pre-planned before flight where vehicle constraints and obstacles can be considered to prevent collisions or entry into no-fly zones. UAVs follow waypoints by implementing guidance algorithms that calculate headings that direct the UAV along a path connecting the waypoints. Obstacles may be discovered during flight that were unknown at initial planning and a new set of waypoints may have to be generated. Waypoints are typically computed at a ground station and are relayed to the UAV by radio, which may be problematic if communication with the UAV is lost. Guidance that accomplishes mission objectives while avoiding obstacles without the need for re-planning waypoints may be beneficial.

Vector Field (VF) guidance is a method that is mainly used for path following and can be useful for obstacle avoidance [W,W,C]. VFs can produce continuous heading vectors that can be used guide a UAV to coverage and follow a path. Vectors are calculated by summing together convergence and circulation terms that are weighted by static scalars. Obstacles can be represented as a path and given a negative convergence weight resulting in a repulsive field. Static repulsive VFs do not always route the UAV around an obstacle. Modifying repulsive VF parameters to be functions of common UAV states could be used to produce an optimal guidance. **The proposed research seeks to determine VF weighting functions that enable optimal obstacle avoidance.**

1.2 Methods Overview

The proposed research will be conducted in three phases where VF guidance singularities will be demonstrated, weighting functions will be investigated, and a developed GVF will be validated on a ground robot simulating a UAV. Phases I and II will be conducted in a simulation environment that combines mission paths and obstacles into a single GVF. Phase III will be conducted with a ground robot simulating a UAV guided by the modified GVF in real-time. Dubin's fixed wing constraints will be imposed in simulations and experiments.

1.3 Phase I

Recreate gradient vector fields for circular and elliptical obstacles and demonstrate singularities. A simulation environment will be built that generates GVFs consisting of mission paths and obstacles. Circular and elliptical obstacles will be investigated and the resulting singularities will be characterized. Static weights will be used and the performance of the guidance measured in distance traveled and time of flight.

1.4 Phase II

Investigate GVF weighting functions that influence obstacle avoidance. UAV closing rate, position, and range will be used to develop dynamic GVF weights for convergence and circulation. The modified GVF will be compared against a static and strictly repulsive GVF. Distance traveled and time of flight will be used to as metrics to compare the modified GVF to the unmodified GVF.

1.5 Phase III

Validate modified GVF model with ground robot experiments. The modified GVF developed in Phase II will be implemented on a differential drive ground robot

simulating a fixed wing UAV. Guidance performance while avoiding static obstacles will be demonstrated.

1.6 Summary of Phases

Each phase consists of an **objective** that will be accomplished by executing *tasks*. Completion of all objectives and phases will result in the final deliverable.

Phase I: Demonstrate Gradient Vector Field Singularities

1. *Build a GVF simulation environment*
2. *Derive GVF for circular and elliptical obstacles*
3. *Identify path and obstacles where singularities are produced*

Phase II: Investigate GVF weighting functions that influence obstacle avoidance

1. *Formulate circulation and convergence weights as functions of UAV state*
2. *Determine combination of GVF weights that produces optimal guidance in simulation*

Phase III: Validate modified GVF model with ground robot experiments

1. *Build differential drive robot*
2. *Build robotic framework to take guidance commands*
3. *Repeat simulations performed in Phase II on ground robot*

Deliverable: Adaptive GVF parameterized weights optimal guidance for path following and static obstacle avoidance.

2 LITERATURE REVIEW

2.1 Introduction to Literature Review

2.2 Unmanned Aerial Vehicle

Unmanned Aerial Vehicles (UAVs) are pilotless aircraft used by military, police, and civilian communities for tasks such as surveillance, reconnaissance, damage assessment, and natural disaster surveying. UAVs are generally categorized into fixed wing and rotor craft varieties that range in size, payload, and flight time capabilities. The aircrafts can be controlled remotely with a RC transmitter or fly on paths connecting pre-planned waypoints. Data can be collected with on-board sensors, such as cameras, which can be stored or relayed to the ground. UAVs are part of an Unmanned Aerial System (UAS) which is made up of the vehicle, autopilot, ground station, transmitter, and two way radio, depicted in Figure 2.1. Ground stations are responsible for monitoring the vehicle's status, planning missions, and generating obstacle free and flyable paths which are sent to the autopilot via two way radio.



Figure 2.1: Unmanned Aerial System (UAS)

The autopilot is responsible for following a pre-planned path and maintaining vehicle stability while under the influence of external wind disturbances. Stable flight while path following is accomplished by implementing feed-back control, navigation, and guidance systems. Feed-back refers to the closure of an open-loop control system which allows an error to be calculated between the desired state of the UAV, the reference, and the current state of the UAV. Reference error is used to calculate the necessary actuator output required to modify the vehicles attitude and position while preventing unbounded oscillations. Feed-back is provided by the navigation system which uses sensors to measure the attitude and position of the aircraft. Sensors often provide noisy data and are sampled at varying rates. Filtering and estimation techniques such as the Kalman filter which fuses and filters measurements to provide an improved state estimation. A high level overview of the autopilots systems can be seen in Figure 2.2.

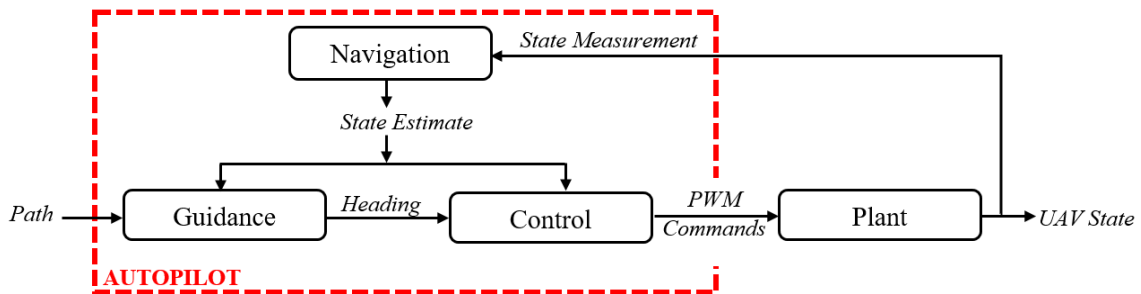


Figure 2.2: Autopilot's Navigation, Guidance, and Control Architecture

The navigation system is responsible for taking high level pre-planned paths from the ground station and providing a reference heading command to the control system. Several methods for path following guidance were investigated in [2] consisting of carrot chasing, non-linear guidance law, pure line-of-sight, linear quadratic regulator, and gradient vector field method. A Monte Carlo simulation with wind disturbances was conducted for the guidance methods above in [2]. It was determined that the vector field method

followed the path with least tracking error and control effort which is the primary goal of path following.

2.3 Vector Field Guidance

2.3.1 Introduction to Vector Field Guidance

- External disturbances - Transitioning to a new state - Avoiding known obstacles - Avoiding pop-up obstacles - Rejecting external disturbances - Computationally inexpensive

Vector field is a continuous guidance method that can be used for guiding a UAV to a singular point or for path following. Potential field and virtual force field guide to a singular point while avoiding obstacles by representing goals and obstacles as artificial attractive and repulsive forces respectively. Path following guidance can be achieved with Lyapunov and gradient vector field techniques that produce heading commands that converge and follow a path.

2.3.2 Potential Field

Potential field is a robotic manipulator method that models a robots workspace as a gradient potential of attractive and repulsive artificial forces [3]. A robot can be represented as a point mass initially located at a globally maximum potential that transitions to a goal located at a globally minimum potential. Obstacles are represented by a high potential that act as repulsive forces with an exponentially decaying strength as to only influence the robot when approaching the obstacle. The potential gradient can be depicted as a mesh such as that shown in Figure 2.3. Potential field is unique in that it combines path planning, trajectory planning, and control into a single system [4].

Inherent problems with potential field methods were identified when experimentally validating the virtual force field (VFF) method in [6]. VFF operates on the artificial attractive and repulsive force principle and is intended specifically for mobile robots

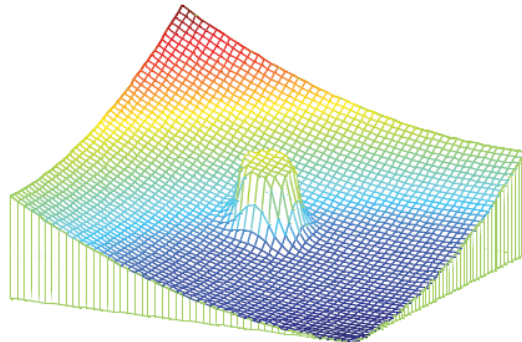


Figure 2.3: Single Obstacle Potential Field Gradient [5]

seeking a goal in an environment with initially unknown obstacles. VFF decomposes a robots workspace into discretized cells that contain an integer certainty value associated with the confidence that an obstacle occupies the cell. A global goal applies an artificial attractive force on the robot that pulls it closer to the goal. As the robot detects obstacles, the certainty value increases in the cell associated with the obstacles position. Cells apply artificial repulsive forces with magnitudes that depend on the certainty value and the distance to the cell.

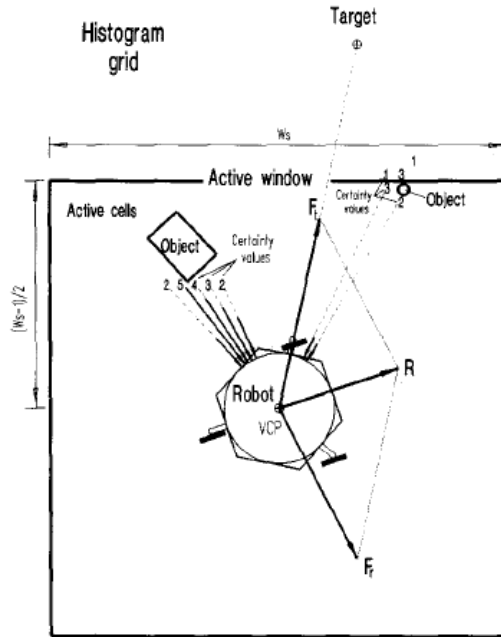


Figure 2.4: Virtual force field histogram acting on a mobile robot

The VFF histogram method was validated on a mobile robot platform using ultrasonic sensors in [7] and [8], avoiding obstacles and seeking a goal. Several problems inherent to all potential field methods were identified while validating the VFF histogram method. Local minimum produced by closely spaced obstacles may create a situation where a robot settles into a lower potential prior to finding the global minimum which is shown in Figure 2.6. Additionally, closely spaced obstacles may also be difficult to pass between, shown in Figure 2.5a. Oscillations can also be experienced near obstacles or in narrow passages at high speeds, shown in Figure 2.5b.

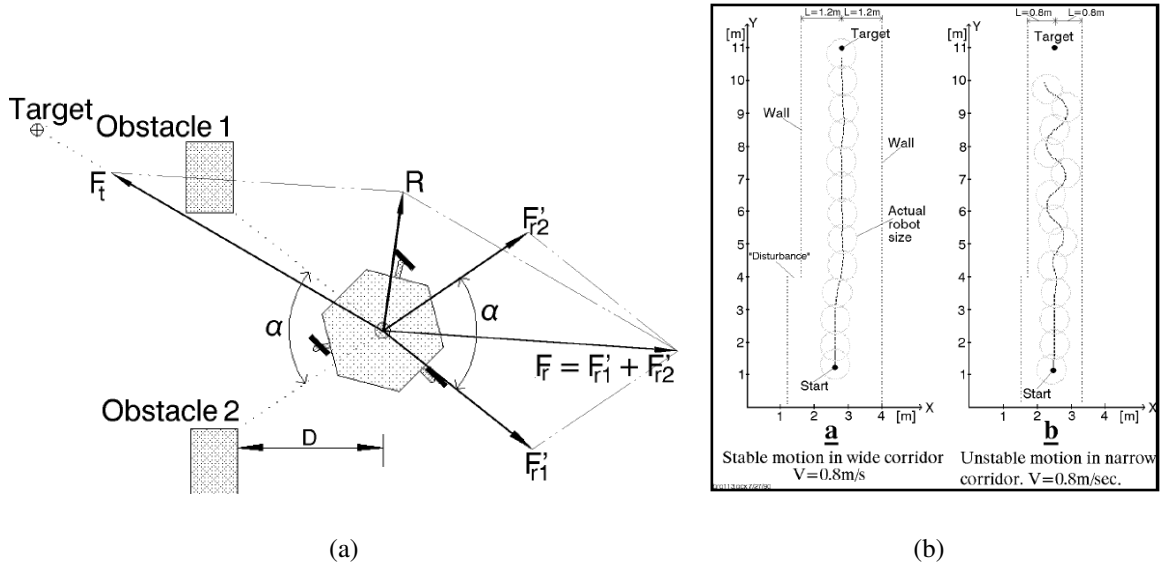


Figure 2.5: Potential Field Local Minimum [5]

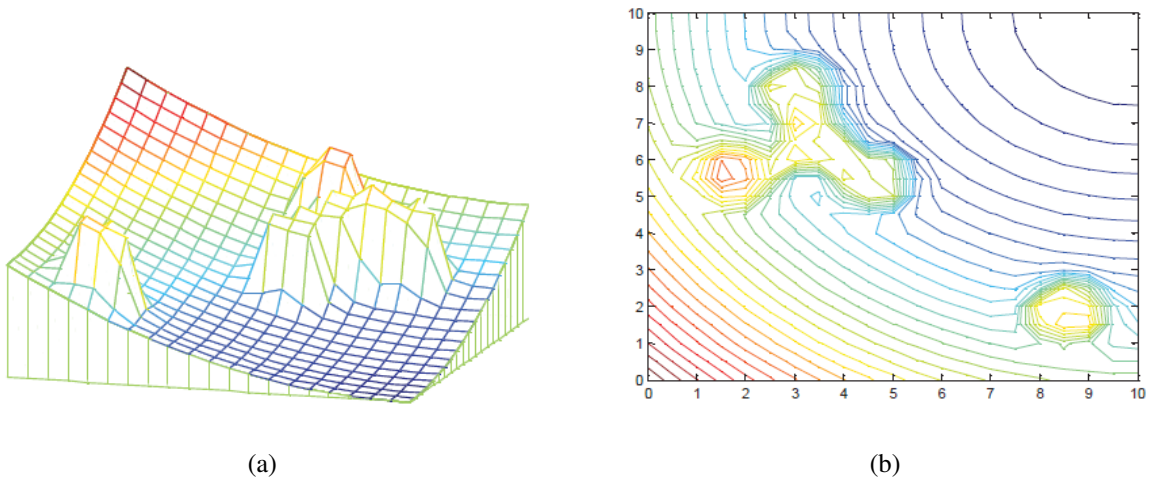


Figure 2.6: Potential Field Local Minimum [5]

Several methods have been developed to eliminate local minimum through the use of navigation functions [9] and obstacle clustering [5]. Navigation functions relate kinematic constraints to the gradient potential to produce a bounded and local minimum free solution [4]. Clustering closely spaced obstacles into a single and equally repulsive

obstacle prevents local minimum from forming. Typical clustering can be seen in Figure 2.7.

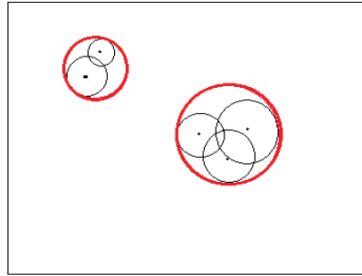


Figure 2.7: Obstacle Clustering [5]

Potential fields ability to avoid obstacles and combine path planning, trajectory planning, and control into a single computationally inexpensive system makes it an attractive motion control system for robots seeking a singular point, even with the limitations discussed in [6]. Unlike ground mobile robots, fixed wing UAVs must maintain a minimum forward velocity and cannot converge to a single point. Vector fields that direct a UAV to paths connecting waypoints have been developed using Lyapunov and gradient vector field techniques.

2.3.3 Lyapunov Vector Fields

Lyapunov vector fields produce heading guidance that asymptotically converges and circulates along a path passing through waypoints. Paths can be built from straight line and circular arc primitives taking UAV dynamic constraints into consideration. Nelson et al. introduced a vector field generation method for line primitives in [10]. Farther away from the path, vectors are constant and point in the direction perpendicular to the path. Within a transition region the vectors begin to rotate and point more parallel to the path. Vectors on the path point directly in the direction of the path. Lyapunov vector fields for straight line and circular arcs are shown in Figure 2.8.

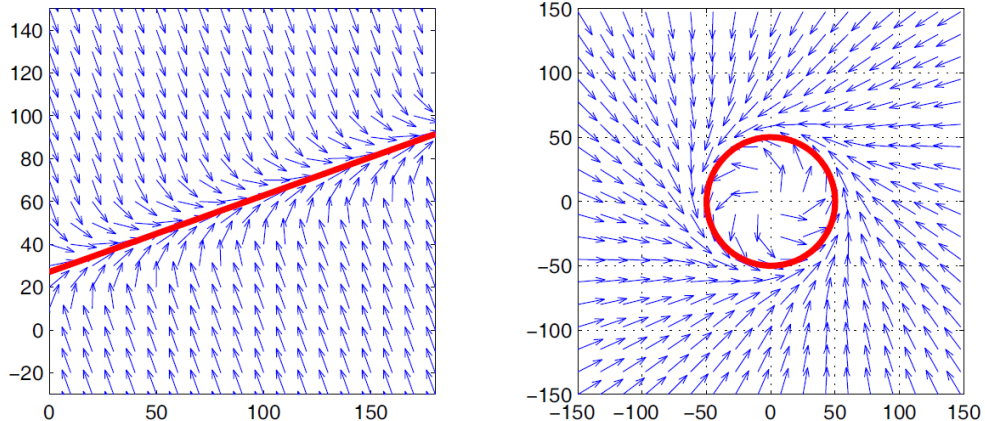


Figure 2.8: Lyapunov vector field for straight line and circular primitives

Combining path primitives together can result in fairly complex paths such as that shown in Figure 2.9. Each path primitive has a vector field associated with it and determining which field to use can be approached in two different ways. Fields from all of the primitives can be summed together similar to the attractive and repulsive forces in potential field. Second, fields can be selectively activated and deactivated based on the position of the UAV. Summing together vector fields, as pointed out in [10], can result in several problems including dead zones, sinks, and singularities. Selectively activating each vector field as a UAV nears waypoints was used in [10] [11] [12].

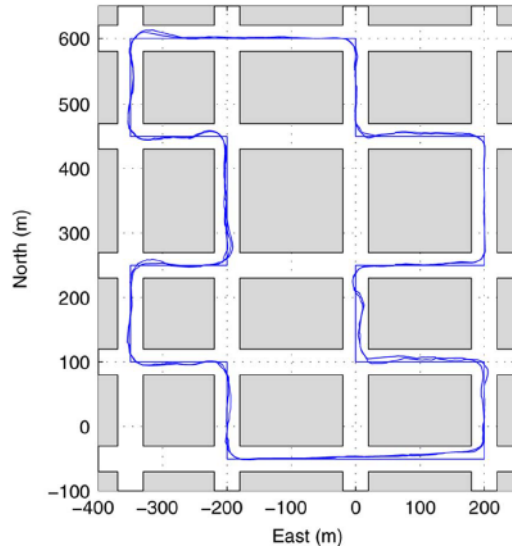


Figure 2.9:

Nelson's method was extended by Griffiths for curved path following and showed that the vectors asymptotically approach the curved path [13], shown in Figure 2.10. Constructing a vector field for an arbitrary curve in place of stitching together primitives has the advantage of not determining which field to activate and may allow for more complex paths.

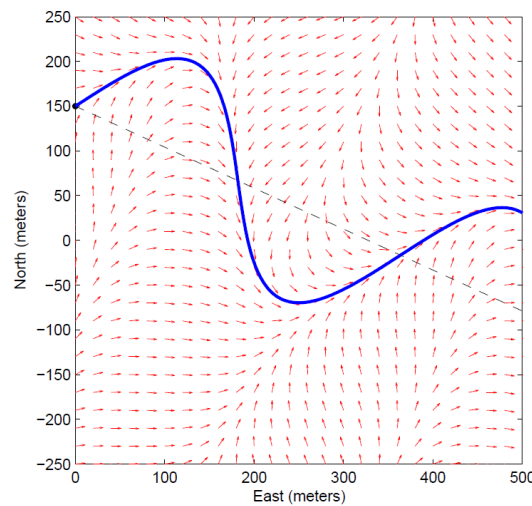


Figure 2.10: Lyapunov vector field approach curved path asymptotically

Primitive circular fields can be modified via non-linear coordinate transformations to produce globally convergent elliptical fields [14] [15]. Frew simulated and experimentally validated the transformed vector field where multiple fixed wing UAVs cooperatively tracked a moving target while maintaining a staggered distance from each other, preventing collision and multiple surveillance angles. The location of a target being tracked is not known with absolute certainty. The covariance matrix from a kalman filter to transform a circular vector field around an uncertain target was investigated in [15] and an example field is shown in Figure 2.11b.

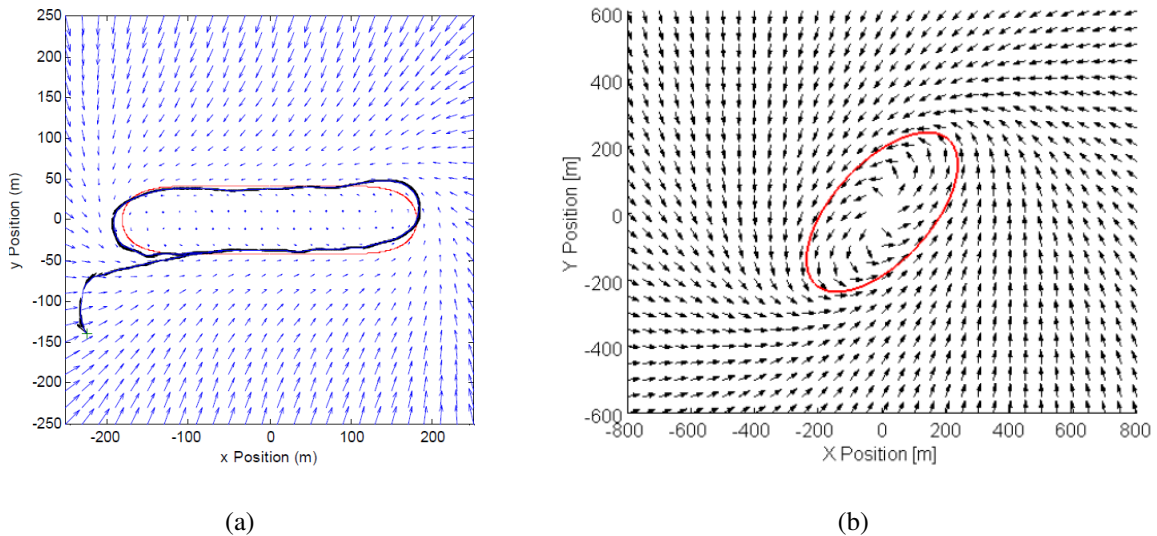


Figure 2.11: Elliptical VF produced by non-linear coordinate transformations a) [14] b) [15]

A target tracking lyapunov plus tangent vector field was introduced in [16] that produced shorter paths compared to lyapunov alone. Outside of the standoff circle, tangent vectors were said to provide the shortest distance to the circle. Inside the standoff circle, no tangent lines exist and lyapunov is used in its place. Figure 2.12 shows the difference in paths taken for lyapunov and tangent vector fields outside the standoff circle. The TPLVF was later used for path planning to avoid obstacles in [17].

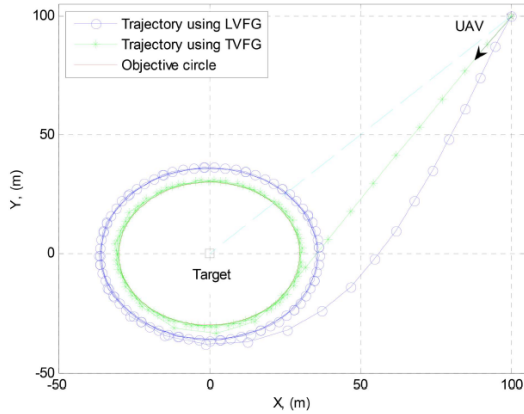


Figure 2.12: Tangent plus lyapunov vector fields for shortest path target tracking [17]

2.3.4 Non-Lyapunov Vector Fields

All methods that consider obstacles so far build a vector field that guides the UAV to an obstacle free path. Another approach is to build a vector field tending to a path and use optimal rapid random trees (RRT*) to explore the space for obstacles and select the optimal path. Pereia et al. developed such a method that builds a tree that makes up possible paths for the UAV to take. Branches extend from the root, or initial location of the UAV, randomly throughout the map with a constrained deviation from the initial vector field. When a branch encounters an obstacle it is trimmed and no longer explored. The path of minimum cost, or least distance, is selected for the UAV to use as a reference path. An example of the algorithm is shown in Figure 2.13.

For well known obstacles in urban environments, such as buildings, an optimal path can be constructed with constrained delaunay triangulation (CDT) which has been previously used in computer animation [18]. CTD was used to construct vector fields in [19] that restricts robots movements inside the triangles while moving towards a global goal. A simulation of a robot traversing a vector field inside a set of CDTs can be seen in Figure 2.14.

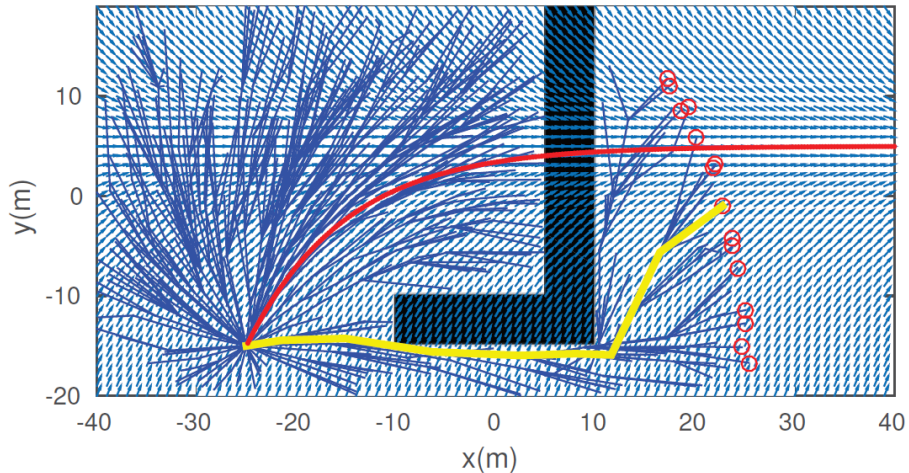


Figure 2.13: RRT* path planner with a VF used as a task specification

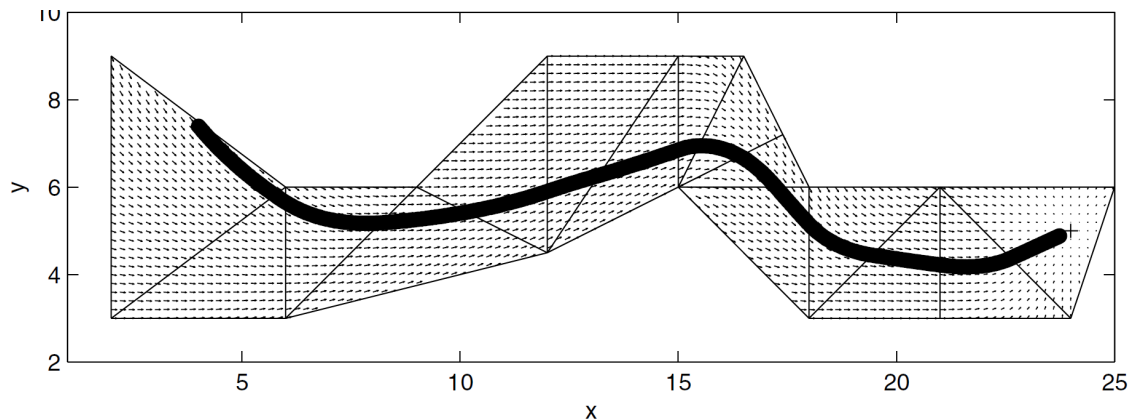


Figure 2.14: Vector field within a set of constrained delaunay triangles [19]

So far all of the vector field methods discussed have avoided obstacles by planning paths around them. Paths are typically calculated at the ground station and if communication is lost a new path may not be relayed to a UAV encountering a new obstacle. A possible solution is using vector fields to provide a repulsive force, not unlike the VFF method, immigrating around the obstacle.

2.3.5 Gradient Vector Field

The gradient vector field method was first introduced in [20] and produces an n -dimensional vector field guaranteed to converge to a path made of points that lie at the intersection of two surfaces. The total vector field \vec{V} is produced by summing together a convergence, circulation, and time varying terms seen in Equation ???. Convergence terms contribute vectors normal to the path, circulation terms contribute vectors parallel to the path, and time varying vectors account for changes in the path as a function of time.

$$\vec{V} = \mathbf{G}\vec{V}_{conv} + \mathbf{H}\vec{V}_{circ} + \mathbf{L}\vec{V}_{tv} \quad (2.1)$$

Each term is multiplied by a scalar, \mathbf{G} , \mathbf{H} , \mathbf{L} , that weights the contribution of each term on the total field \vec{V} . Only static paths will be discussed so it is assumed the time varying field is null. The advantage of GVF is the convenient access to the weighting terms that independently effect the total field. Magnitude of the weights modifies the strength of each fields influence, whereas the sign indicates the direction. Figure 2.15 shows convergence and circulation fields for a circular path where the weights \mathbf{G} and \mathbf{H} are unity and positive. The convergence field contains vectors that are normal to the circular path for all points in space, with exception to the center of the circle which is undefined. Circulation fields contain vectors that are parallel to the path for all points in space with the same exception of no definition at the center of the circle.

Modifying the signs of \mathbf{G} and \mathbf{H} to be unity and negative results in similar fields but with a 180° rotation about the center of the circle, Figure 2.16. The attractive convergence field becomes a repulsive field, where all vectors are anti-normal to the path. The circulation field changes direction and rotates counterclockwise around the path.

Repulsive fields have been used for obstacle avoidance for a UAV loitering around a moving target in [w,w,c]. A circular goal path was attached to a ground vehicle and a

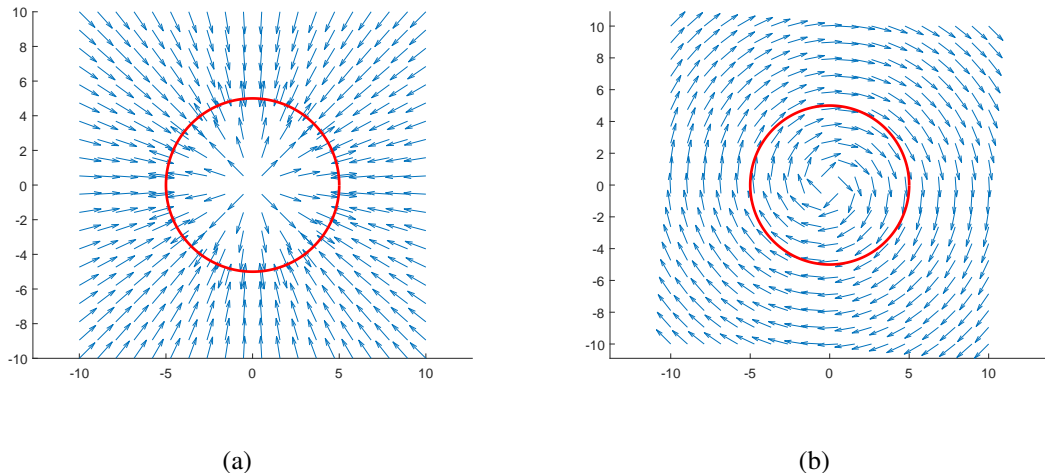


Figure 2.15: Attractive vector field (a) and clockwise circulation field (b)

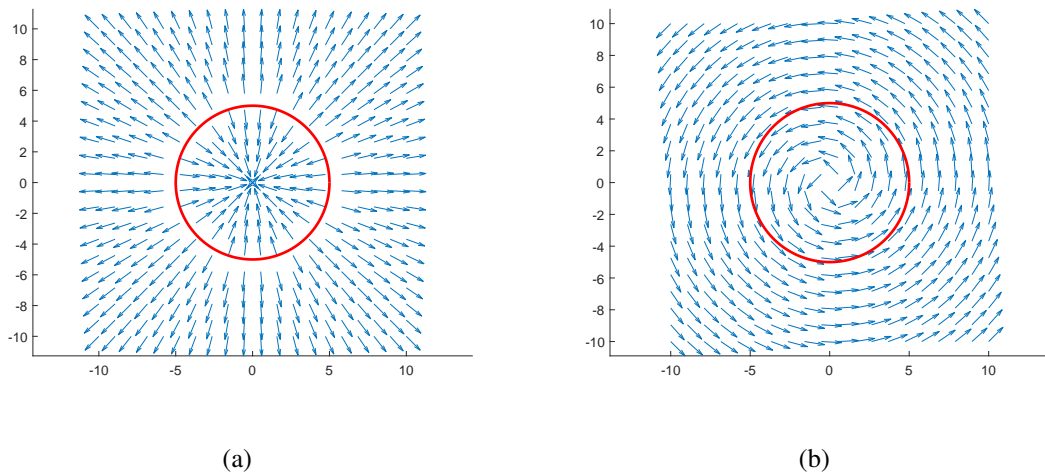


Figure 2.16: Repulsive vector field a) and counterclockwise circulation field b)

convergence and circulation vector field was generated. Circular paths were with small radii were placed on top of obstacles with strictly repulsive weights. Notice in Figure 2.16a that inside of the path, vectors guide inward, which is not desired for obstacle avoidance. The problem is alleviated by reducing the radius significantly. Goal and obstacle field are

summed together to provide a total field that provides guidance to a UAV. Loitering is accomplished while avoiding two obstacles, as shown in Figure 2.17

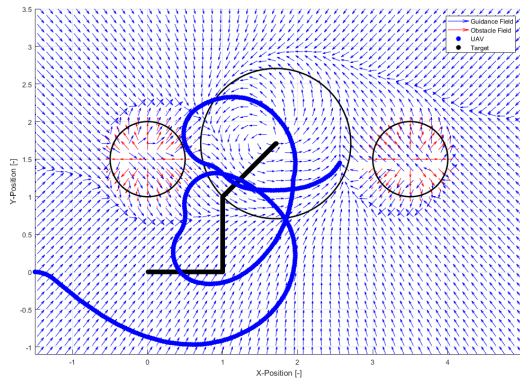


Figure 2.17: Place holder image of UAV following ground target

Similar to potential field and VFF, the strength of the repulsive field depends on the distance from an obstacle. In [w,w,c], a tangent hyperbolic decay function was assigned to the obstacle fields which varied the total strength from null to unity, shown in Figure 2.18.

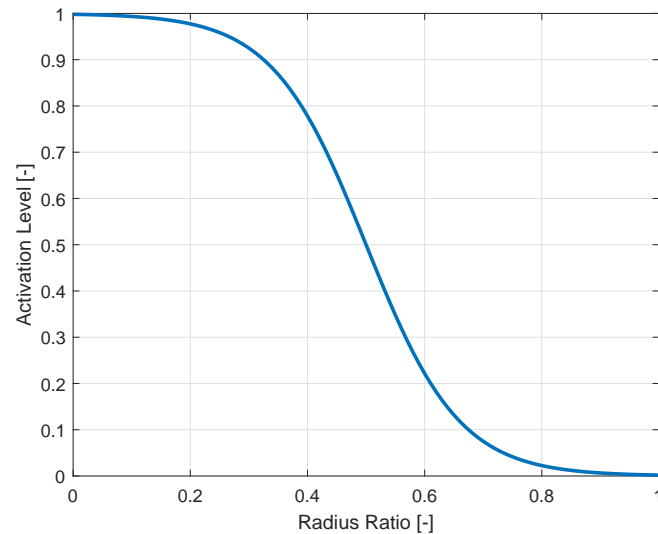


Figure 2.18:

Constructing the paths for a UAV flying at constant altitude requires three-dimensional surfaces intersecting to form two-dimensional paths. Consider a UAV in 2-dimensional space tracking a path τ , which is made of points that lie at the intersection of two surfaces. Each of the surfaces α_i is continuous, differentiable, and is a function of the set $q = [x, y, z]$. The convergence field \vec{V}_{conv} is produced by the sum of surfaces multiplied by their respective partial gradient $\nabla_q \alpha_i$. The definition of the convergence field is summarized in Equations 2.2 and 2.3.

$$\vec{V}_{conv} = \mathbf{G} \sum_{i=1}^{n-1} \alpha_i \nabla_q \alpha_i \quad (2.2)$$

$$\nabla_q = \begin{bmatrix} \frac{\partial}{\partial x} \\ \frac{\partial}{\partial y} \\ \frac{\partial}{\partial z} \end{bmatrix} \quad (2.3)$$

To produce a circular path of radius r the intersection of a cylinder and plane are used, as shown in Equations 2.4-2.5 and pictured in Figure 2.19.

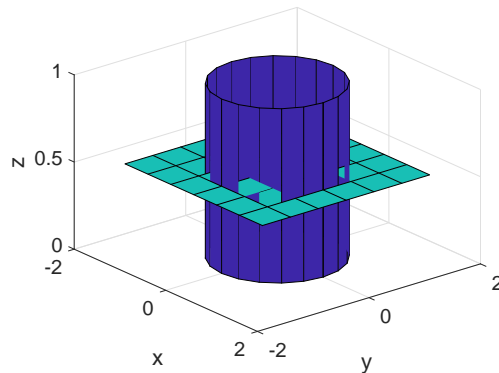


Figure 2.19:

$$\alpha_1 = x^2 + y^2 - r^2 \quad (2.4)$$

$$\alpha_2 = z \quad (2.5)$$

Convergence vector field term is produced by taking the wedge product of the partials $\nabla_q \alpha_i$, which in three dimensions simplifies to the cross product as shown in Equations 2.6 and 2.7.

$$\vec{V}_{circ} = \mathbf{H} \wedge_{i=1}^{n-1} \nabla_q \alpha_i \quad (2.6)$$

$$\vec{V}_{circ} = \mathbf{H}(\nabla_q \alpha_1 \times \nabla_q \alpha_2) \quad (2.7)$$

Circulation and convergence terms may have different magnitudes depending on the location of origin of a vector and the equations used for surfaces. Normalizing each component prior to weighting allows for more predictable results when assigning values. So far the VF weights have been used for high level specification of the desired behavior for a UAV, whether it be for convergence, avoidance, or circulation. Furthermore, there is no guarantee that when using a vector field for avoidance that the UAV will not violate the no-fly zone. If the UAV turn rate is at saturation an increased reference command will do nothing to aid in avoidance. A demonstration of saturation is seen in Figure 2.20 where a UAV is provided guidance by a convergent and circulating vector field about a circular path.

If the VF was adjusted earlier at an earlier state, the tracking error may be reduced. When using an obstacle, determining which direction the UAV must fly around the obstacle is important to reduce distance flown. Determining functions for the sign and magnitude of the vector field weights to produce an optimal guidance.

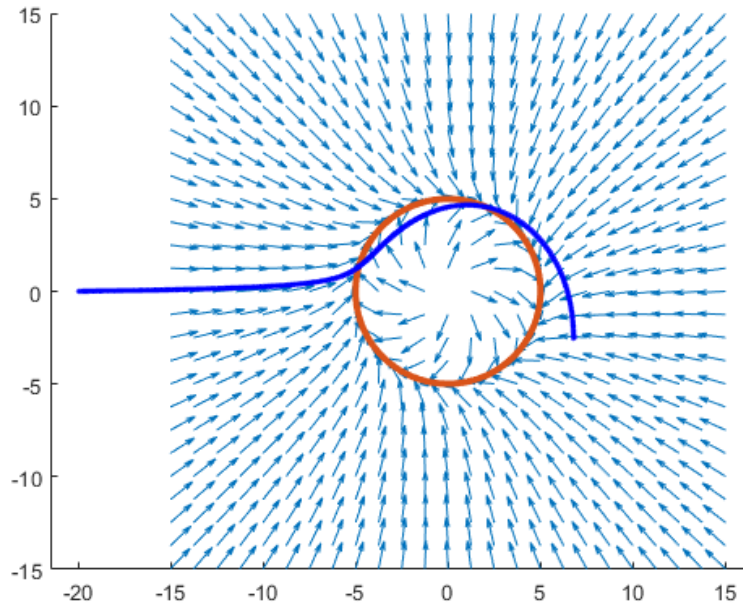


Figure 2.20: Dubins UAV actuator saturation

2.4 Unmanned Aerial Vehicle Simulation

Testing new guidance, navigation, and control algorithms can be costly, require significant time, and requires an adequately large airspace. Ground stations need to be established which require power and shelter. Some small fixed wing UAVs may not be suitable to fly in all weather, therefore test flights may be canceled due to weather conditions. Lastly, larger UAVs need to have FAA clearance before flight which has to be pre-approved and takes time. Before spending the time to reserve airspace and allocate man hours for flight tests it is important to test algorithms in a controlled environment. One way to accomplish testing without actual flight is through validation through mobile robots simulating fixed wing constraints [21], [22], [23]. Programming a mobile robot, such as one shown in Figure

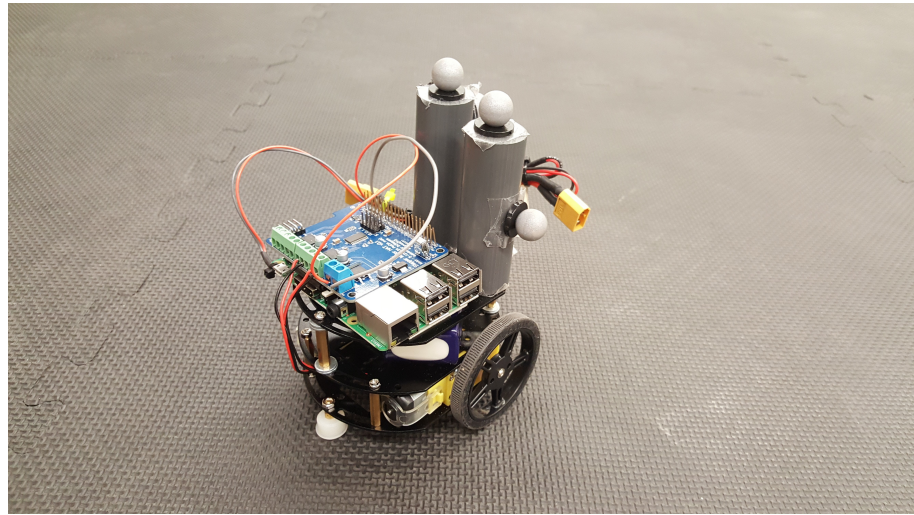


Figure 2.21: Differential drive mobile robot simulating fixed wing UAV Dubins constraints

2.5 Literature Review Summary

•

REFERENCES

- [1] Bone, E., “UAVs backbround and issues for congress.pdf,” 2003.
- [2] Sujit, P., Saripalli, S., and Sousa, J. B., “Unmanned Aerial Vehicle Path Following: A Survey and Analysis of Algorithms for Fixed-Wing Unmanned Aerial Vehicless,” *IEEE Control Systems*, Vol. 34, No. 1, Feb. 2014, pp. 42–59.
- [3] Khatib, O., “Real-time obstacle avoidance for manipulators and mobile robots,” *The international journal of robotics research*, Vol. 5, No. 1, 1986, pp. 90–98.
- [4] Rimon, E., “Exact Robot Navigation Using Artificial Potential Functions.pdf,” 1992.
- [5] Liu, Y. and Zhao, Y., “A virtual-waypoint based artificial potential field method for UAV path planning,” *Guidance, Navigation and Control Conference (CGNCC), 2016 IEEE Chinese*, IEEE, 2016, pp. 949–953.
- [6] Koren, Y. and Borenstein, J., “Potential Field Methods and their inherent limitions for mrobile robot navigation.pdf,” 1991.
- [7] Borenstein, J. and Koren, Y., “Real-time obstacle avoidance for fast mobile robots in cluttered environments,” *Robotics and Automation, 1990. Proceedings., 1990 IEEE International Conference on*, IEEE, 1990, pp. 572–577.
- [8] Borenstein, J. and Koren, Y., “The vector field histogram-fast obstacle avoidance for mobile robots,” *IEEE transactions on robotics and automation*, Vol. 7, No. 3, 1991, pp. 278–288.
- [9] Goerzen, C., Kong, Z., and Mettler, B., “A Survey of Motion Planning Algorithms from the Perspective of Autonomous UAV Guidance,” *Journal of Intelligent and Robotic Systems*, Vol. 57, No. 1-4, Jan. 2010, pp. 65–100.
- [10] Nelson, D. R., “Cooperative control of miniature air vehicles,” 2005.
- [11] Nelson, D. R., Barber, D. B., McLain, T. W., and Beard, R. W., “Vector field path following for small unmanned air vehicles,” *American Control Conference, 2006*, IEEE, 2006, pp. 7–pp.
- [12] Nelson, D., Barber, D., McLain, T., and Beard, R., “Vector Field Path Following for Miniature Air Vehicles,” *IEEE Transactions on Robotics*, Vol. 23, No. 3, June 2007, pp. 519–529.
- [13] Griffiths, S., “Vector Field Approach for Curved Path Following for Miniature Aerial Vehicles,” American Institute of Aeronautics and Astronautics, Aug. 2006.
- [14] Frew, E., “Lyapunov Guidance Vector Fields for Unmanned Aircraft Applications.pdf” .

- [15] Frew, E. W., “Cooperative standoff tracking of uncertain moving targets using active robot networks,” *Robotics and Automation, 2007 IEEE International Conference on*, IEEE, 2007, pp. 3277–3282.
- [16] Chen, H., Chang, K., and Agate, C. S., “Tracking with UAV using tangent-plus-Lyapunov vector field guidance,” *Information Fusion, 2009. FUSION'09. 12th International Conference on*, IEEE, 2009, pp. 363–372.
- [17] Chen, H., Chang, K., and Agate, C. S., “UAV path planning with tangent-plus-Lyapunov vector field guidance and obstacle avoidance,” *IEEE Transactions on Aerospace and Electronic Systems*, Vol. 49, No. 2, 2013, pp. 840–856.
- [18] Md, Z., Rg, C., and Dj, G., “Simplex Solutions for Optimal Control Flight Paths in Urban Environments,” *Journal of Aeronautics & Aerospace Engineering*, Vol. 06, No. 03, 2017.
- [19] Pimenta, L. C., Pereira, G. A., and Mesquita, R. C., “Fully continuous vector fields for mobile robot navigation on sequences of discrete triangular regions,” *Robotics and Automation, 2007 IEEE International Conference on*, IEEE, 2007, pp. 1992–1997.
- [20] Goncalves, V. M., Pimenta, L. C. A., Maia, C. A., and Pereira, G. A. S., “Artificial vector fields for robot convergence and circulation of time-varying curves in n-dimensional spaces,” IEEE, 2009, pp. 2012–2017.
- [21] Ren, W., McLain, T., Sun, J.-S., and Beard, R., “Experimental validation of an autonomous control system on a mobile robot platform,” *IET Control Theory & Applications*, Vol. 1, No. 6, Nov. 2007, pp. 1621–1629.
- [22] Louali, R., Djouadi, M. S., Nemra, A., Bouaziz, S., and Elouardi, A., “Designing embedded systems for fixed-wing UAVs: Dynamic models study for the choice of an emulation vehicle,” IEEE, Feb. 2014, pp. 1–6.
- [23] Louali, R., Elouardi, A., Bouaziz, S., and Djouadi, M. S., “Experimental Approach for Evaluating an UAV COTS-Based Embedded Sensors System,” *Journal of Intelligent & Robotic Systems*, Vol. 83, No. 2, Aug. 2016, pp. 289–313.